COMPARATIVE GEOMETRIC TESTS OF INDUSTRIAL AND SCIENTIFIC CCD CAMERAS USING PLUMB LINE AND TEST RANGE CALIBRATIONS

Mark R. Shortis

Department of Geomatics
The University of Melbourne
Parkville, Victoria 3052, AUSTRALIA
Telephone : +61 3 344 6806
Facsimile : +61 3 347 2916
M.Shortis@unimelb.edu.au

Walter L. Snow and William K. Goad

Experimental Testing and Techniques Division
NASA Langley Research Center
Hampton, Virginia 23665, U.S.A.
Telephone : +1 804 864 4613
Facsimile : +1 804 864 7607
W.L.Snow@larc.nasa.gov
W.K.Goad@larc.nasa.gov

KEY WORDS : Calibration, CCD, Plumb line, Test range, Sensor geometry

ABSTRACT

Small format, medium resolution CCD cameras are at present widely used for industrial metrology applications. Large format, high resolution CCD cameras are principally used for scientific applications, but are slowly infiltrating photogrammetry and dramatically improving the object space accuracy achievable by close range measurement. The calibration of all types of CCD cameras is necessary in order to characterise the geometry of the sensors and lenses. Fourteen different types of CCD sensor and lens combinations have been calibrated at the NASA Langley Research Center using plumb line calibration combined with self-calibration and a targeted test field. The results of these calibration tests will be described, with particular emphasis on the dependence on sensor resolution and a comparison of industrial and scientific CCD cameras.

1. INTRODUCTION

Camera calibration has been and will always be a necessary part of the photogrammetric process. Knowledge of the internal geometry of the camera is essential if the principle of collinearity is to be correctly applied. Without this knowledge, derived measurements in the object space will be affected by systematic errors and therefore will be degraded in accuracy. Whilst in many circumstances self-calibration may be feasible, in some cases such an approach is not appropriate. Self-calibration is typically ruled out because the geometry of the photogrammetric network is too weak to determine the calibration parameters with confidence or with a reasonable degree of independence. The internal characteristics of the camera must therefore be determined before or after the actual measurement process, or preferably both.

Since their introduction in the 1970s, CCD cameras and digital images have gained wide acceptance for machine vision and industrial metrology. The very nature of the tasks in which CCD cameras are employed tends to exacerbate rather than ameliorate the calibration problem. Real time or near real time applications require multiple, fixed (and synchronised) cameras (Childers et al, 1994), whereas self-calibration is most effective with a single, portable camera (Fraser and Shortis, 1995). Further, such applications often involve small numbers of targets, whereas a dense, three dimensional array of targets which fills the camera format vastly increases the effectiveness of self-calibration.

Pre- or post-calibration can be carried out by a variety of techniques. Using an established test field, comprising a two or three dimensional array of suitable targets with known coordinates, and multiple photographs is perhaps the most common method and has been used for virtually all types of cameras (Earls, 1983; Merchant and Tudhope, 1989; Wiley and Wong, 1995). However, known target coordinates may not be necessary. If the geometry of the photogrammetric network is sufficient (Shortis and Hall, 1989) and only the primary physical calibration parameters (principal point, principal distance, lens distortions, image orthogonality and image affinity) are desired then the situation reverts to a self-calibration. The calibration is in effect taking advantage of a better network geometry which can not be obtained during operational photography. Although it is advisable to include an accurate distance between two targets to correctly scale the network, even this minimum information is unnecessary for self-calibration.

Other techniques are generally partial calibrations which derive a subset of parameters. The plumb line calibration method was originally developed by Brown (1971) for close range cameras, but has been successfully and routinely applied to aerial (Hentschel and Shortis, 1991), tube type video (Burner et al, 1985) and CCD video cameras (Fryer and Mason, 1989). This technique is capable of deriving the lens distortion parameters independently from all other parameters, and can be carried out under operational conditions. Many specialised techniques have been developed to empirically or analytically derive particular aspects of the internal geometry of cameras. For example, Lenz (1987) used target tracking to determine the principal point location and a 2D point array to determine radial distortion of a zoom lens on a CCD camera, the DLT approach to combined exterior and interior orientation of cameras is widely used (Burner et al, 1985) and simple techniques have been developed for non-specialists to obtain a minimal calibration (Snow et al, 1993).

2. CCD CAMERA CALIBRATION AT NASA LANGLEY RESEARCH CENTER

Close range photogrammetric techniques have been in use at NASA Langley Research Center (LaRC) for almost twenty years. Photogrammetric techniques for wind tunnel testing initially used synchronous stereophotography with

conventional non-metric cameras to measure deformations of wind tunnel models under test conditions (Brooks and Beamish, 1977). More recently, state of the art, large format, metric cameras have been routinely used to characterise large space structure components using self-calibration (Shortis, 1989). In parallel with the film-based photogrammetry, research at LaRC has also focussed on utilising CCD based systems to provide access to hostile environments and to capture dynamic events. Initial experiments utilised analog video cameras (Burner et al, 1985), but these were quickly replaced with solid state cameras to avoid vibration, environmental and interference problems often encountered with applications in wind tunnels. Burner et al (1987) describes the evolution of a CCD camera system currently installed in the National Transonic Facility. Childers et al (1994) describes a recent application of CCD cameras to characterise the motion of a free-flight model in a large wind tunnel.

The requirement for pre- and/or post-calibration of CCD cameras at LaRC is a direct result of applications such as wind tunnel testing. The placement of cameras and target arrays is severely limited within the test zones of wind tunnels and self-calibration is rarely possible due to the constraints on network geometry. To capture the images in real time during model tests there is mandatory requirement for multiple, fixed cameras, so simple resection/intersection techniques are in use at LaRC as appropriate to the task at hand. However, there is continuous demand on wind tunnel instrumentation to improve the accuracy of measurement in accord with more stringent engineering tolerances. The modelling and elimination of systematic errors in the complete image capture and measurement process, including the deterioration caused by, for example, recording media (Shortis et al, 1993), is an integral part of all CCD camera processing at LaRC.

3. THE CALIBRATION APPROACH

The use of target fields to calibrate CCD cameras has been successfully implemented by a number of researchers (Beyer, 1987; Bösemann et al, 1990; Gustafson, 1988). In order to confidently derive the calibration parameters, the geometry of the network should be essentially the same as that required for self-calibration. Multiple, convergent photographs of the target field are taken, preferably with a range of camera to object distances and a variety of roll angles to reduce correlations between parameters. The calibration parameter set typically comprises primary physical parameters to model the imaging system characteristics and high-order additional parameters to model image non-linearities and image plane unflatness (Faig and Shih, 1988). The target images are observed manually or measured by digital image processing semi-automatically and the network analysis is based on the principle of collinearity and an iterative solution by least squares estimation (Shortis, 1989; Shortis et al, 1991).

However, self-calibration of CCD cameras using the targeted test field technique does have potential problems. The small size of the sensor area and the relatively long principal distances give rise to strong correlations between internal and external orientation parameters. Typical of these is the projective coupling between the principal point location, decentring distortion and (for example) the tip and tilt of the camera, as small changes to any of these parameters results in similar changes within the image space. Parameter constraint is the usual remedy, taken to the extreme of parameter suppression in some cases. Because it is rare for two parameters to be 100% correlated there is always some unavoidable degradation of the accuracy from the network adjustment, caused by unmodelled systematic errors.

To reduce the level of correlation internally between the primary physical parameters, and between these parameters and external orientation parameters, an initial plumb line calibration can be carried out. As previously mentioned, a plumb line calibration obtains the lens distortion parameters effectively independently of all other calibration parameters. The results of the plumb line calibration can be used to constrain the subsequent self-calibration. Parameter constraints are conveniently incorporated into the least squares estimation process via sequential adjustment, also known as à priori weights (Case, 1961).

There are two restrictions which must be placed on the rigorous implementation of a combined calibration approach. First, the plumb line calibration is not totally independent of the results of the self-calibration. The location of the principal point, as well as any non-linearities or unflatness of the sensor, must be considered. As the lens distortions are computed relative to the principal point, any substantive error in the assumed location will affect the results and invalidate the constraints applied to the self-calibration. Non-linearities or unflatness of the sensor will similarly affect the plumb line calibration, albeit at a much lower level, and must be accounted for in the analysis. The strategy which must be adopted, in the absence of an integrated solution, is an iterative computation. The plumb line data is first analysed using an assumed principal point location. The computed lens distortion data is then used as constraints in the self-calibration network computation. The principal point coordinates are updated and any significant high order calibration parameters are incorporated into a re-computation of the plumb line calibration. The results of this second computation of the plumb line calibration are then used as constraints in a second self-calibration network computation. The iteration process, in most cases, will be short-lived. Exceptions will be experienced only when the initial knowledge of the camera and sensor is grossly erroneous.

Second, the plumb line and self-calibration images must be recorded at the same focus setting and within a reasonable time delay in order to characterise the lens whilst it is a consistent state. It is also worthy of note that the plumb line images would normally have a single plane of focus, whilst self-calibration images of a test range are likely to have a significant depth of field due to the three dimensional nature of the test range or the convergent photography, or both. This raises the issue of change in lens distortion for test field targets imaged out of the plane of focus. However, due to the small size of the CCD sensors and relatively long focal length lenses used in this study, the magnitudes of the lens distortions are generally small, which should lead to commensurately small changes in lens distortion out of the plane of focus (Fraser and Shortis, 1992).

4. CAMERA TYPES

Fourteen different types of CCD sensor and lens combinations have been calibrated at LaRC using the technique. The characteristics of these cameras are shown in Table 1. The first six cameras could be considered "off-the-shelf", low resolution CCD sensors typically used for industrial or machine vision applications. The sensors are based around the CCTV diagonal dimension formats and, with one exception, transfer the video images via 14.3MHz RS-170 analogue signals. Both interline transfer and frame transfer read-out type sensors are represented. The images from these cameras were acquired using an Epix Silicon Video frame grabber. Pixelsynchronous transfers were not used for analogue transmissions, as this facility was not available for all of these cameras. The exception in this group is the Cohu digital camera, which has a non-standard digital interface for connection to a special adaptor board for the Epix frame grabber. This is effectively a pixelsynchronous transfer and avoids the uncertainties, such as line jitter and transfer losses (Beyer, 1987), associated with RS-170 analogue transmission.

CCD Camera	Sensor Format or Type	Grey Level Range	Horizontal Pixels	Vertical Pixels	Horizontal Spacing (um)	Vertical Spacing (um)	Focal Lengths (mm)
Elmo EM-102BW	1/2" interline	256	752	480	8.5	10.0	15
Sony XC999	1/2" interline	256	752	480	8.5	9.7	12.5
Cohu 4810 analogue	2/3" frame	256	752	480	11.5	13.5	12.5
Cohu 4810 digital	2/3" frame	256	752	480	11.5	13.5	12.5
Hitachi KP-M1	2/3" interline	256	752	480	11.0	13.0	12.5
Pulnix TM-845	2/3" frame	256	752	480	11.5	13.5	12.5
TI Multicam MC-1134GN	2/3" frame	256	1104	936	7.8	6.8	12.5
Thompson TH31156-L2	Scientific	16384	1024	1024	19.0	19.0	24, 50
Kodak KAF 1400	Scientific	4096	1035	1320	6.8	6.8	24, 50
Kodak 4.2 Megaplus	Scientific	256	2028	2044	9.0	9.0	24, 50
Kodak DCS200ci	Still video	3x256	1524	1025	9.0	9.0	28

Table 1. Characteristics of the calibrated CCD cameras

All the remaining cameras contain medium to high resolution sensors requiring specific interfaces which vary from the standard, analogue RS-170 transmission. The Texas Instruments Multicam has a multi-mode feature, and for the experiments described here the maximum resolution mode was selected. This is a "pseudo-interlace" mode which effectively doubles the vertical resolution of the sensor, compared with the standard mode. The video images from the camera are transmitted using an analogue signal, but at the relatively high frequency of 43MHz.

The Elmo and Sony cameras are physically small and utilise micro-lenses. The next five cameras in Table 1 are somewhat larger and all will accept C-mount type CCTV lenses. Calibration of a number of sensors with the same lens raised the possibility of testing the stability of the lens distortion parameters, which should be independent of the sensor type. Accordingly, a 12.5mm Fujinon lens was used with approximately the same focus setting in all cases except the Cohu digital camera. An exact duplication of the focus setting could not be guaranteed due to the different back-focus requirements for the different camera bodies and the need to focus accurately on the target field.

The Thompson and Kodak 1400 cameras are high quality sensors mounted in thermo-electrically cooled housings thereby affording slow-scanning (50-200 kHz) and low noise read-out. The digital output further improves noise and minimises sampling errors. The Kodak 4.2 Megaplus camera uses the highest pixel density sensor available at the time of the tests, has a digital output and a relatively slow read-out of 500 kHz. The Thompson and Kodak 1400 cameras used a Photometrics interface/controller and the Kodak 4.2 Megaplus used a Macintosh based data acquisition system. These cameras have several functional differences, compared to standard video cameras, which make them more difficult to operate and use. Apart from the much larger image files produced, a complete image from the Thompson sensor, for example, requires approximately 20 seconds to acquire, so focussing must be accomplished using only a small part of the image. The KAF 1400 sensor has now been re-packaged as the Megaplus 1.4 camera.

It is well known that increased radiometric precision improves the precision of target location in digital images (Trinder, 1989). Although it could be argued that geometric and radiometric performance of CCD sensors cannot, and perhaps should not, be tested in isolation, the intent here was to carry out a comparison of the geometric performance only. A further justification for the emphasis on geometric evaluation is that the calibration images would be close to binary in nature (high grey values against a minimal background), which would reduce the influence of radiometric resolution.

The Thompson and both Kodak camera housings are physically quite large and utilise F-mount type lenses. Again, calibration of a number of sensors with the same lens was possible and all three cameras were calibrated with the same 24mm Nikkor lens. The opportunity was also taken to calibrate the Thompson and the Kodak 1400 cameras with two lenses of different focal lengths. Calibration of the same sensor with multiple lenses raises the possibility of testing the stability of the affine scale and orthogonality parameters derived for the sensor, which should be independent of the lens type. The Kodak 4.2 camera was calibrated with two different lenses due to problems with the first attempt at

image acquisition.

The last camera shown in Table 1 is the Kodak DCS200 and is classified as a still video camera because of its portability and on-board storage of images (Fraser and Shortis, 1995). Data transfers are digital in nature via a SCSI interface, which in theory completely excludes problems such as line jitter and transmission errors. At the time of the experiment a monochrome version of this camera was not available and a colour version was tested, however it was proposed that the GRGBGRGB.... horizontal line sequence on the sensor might be deconstructed from the 24 bit RGB image produced by the camera. For the sake of expediency, the 24 bit colour images were simply band-averaged to 8 bit grey scale images. Unfortunately this double re-processing of the raw pixel values proved to be not a true test of the sensor.

5. DATA ACQUISITION AND PROCESSING

Eight frames of a targeted test field were taken with each camera. The geometry of the network adhered to the optimal ring configuration and 90° convergence proposed by Fraser (1986), in every case. The camera was rolled about the optical axis by 45° after each frame. The camera to object distance was set in each case as a compromise between maximum coverage within the format of the sensor and minimal target image losses at the edge of the frame due to changes in perspective and camera roll.

The target field is a black aluminium plate with an array of 121 passive targets, which are a mixture of targets flush with the surface and stand-off targets on rods. The target field encloses a volume of 0.5m by 0.5m by 0.25m. Passive targets were adopted to avoid the response fall off of retro-reflective targets at high incidence angles. In every case the cameras and the test field were allowed at least two hours to reach thermal equilibrium before the calibration test commenced. Data acquisition required, on average, 20 minutes. Typically the laboratory temperature is stable to better than 1°C over such short periods of time, hence it is extremely unlikely that the plate would change significantly in shape during the time required for a calibration test.

Using the same focus setting and camera to object distance, three or four frames of a plumb line calibration range were taken with each camera. Again, the camera was rolled about the optical axis by 45° after each frame. The plumb lines are white plastic cords, under tension, against a black background. A mixture of overhead and auxiliary lighting was used for the targeted object and the plumb lines. The grey levels were monitored to maximise the target or plumb line signal, and minimise the background, whilst avoiding saturation of the sensor. Pixel intensities in the target field frames averaged 200 and 5 for the target images and the background, respectively. The target images spanned 7 and 30 pixels on average for the low and high resolution sensors respectively. Pixel intensities in the plumb line range frames averaged 150 and 20 for the plumb line images and the background, respectively. The plumb lines spanned approximately 4 and 12 pixels on the low and high resolution sensors respectively. Typical images are shown in Figure 1.

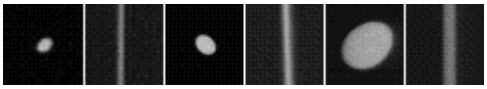

Figure 1. Target and plumb line images from (left to right) low, medium and high resolution sensors. All image windows are from near the centre of frame and are 40 pixels square.

The target images are located within the frame using a semi-automated procedure based on the known object space coordinates of the targets and a resection/intersection computation (Shortis et al, 1991). Each 8 frame data set comprised approximately 900 target images. Positions on the plumb lines were gathered using a semi-automated procedure based on simple line following. Measurement of each frame produced approximately 20 locations on 20-35 plumb lines, leading to a total ranging between 1500 and 2500 image locations from the four frame sets.

Because of the high signal to background ratio and the uniformity of the background, thresholds were set by a simple additive constant of 5 grey levels above the background. The weighted centroid of the target or plumb line image was then computed using the non-zero intensity pixels inside the window (Trinder, 1989). More complex image location schemes, such as template matching or intensity profiles, were not warranted here because of the binary nature of the images supplied by the targets and plumb lines (Shortis et al, 1994).

Initially, only one set of frames was acquired with the Kodak Megaplus 4.2 camera, using the 24mm lens. During the processing of the images it became apparent that there was read-out noise in the frames of the test field. The "comet tails" were not readily visible in the original images and were only shown clearly in a contrast enhanced image. A number of strategies were employed to overcome the affect of the noise, such as different threshold algorithms and ellipse fitting instead of centroiding, but no improvement could be achieved in the subsequent calibration computations. A few months later the camera was again loaned to LaRC and another set of images was acquired, in this case with a 50mm lens and only of the target field. No significant read-out noise could be detected in these frames.

The image data from the CCD cameras was processed using the CRAMPA suite of programs (Shortis, 1989) executed on an IBM compatible PC. All plumb line calibration data sets were initially processed using a principal point at the centre of the frame and no high order additional parameters to model non-linearities or sensor unflatness. All target field data sets were then treated as self-calibrating free networks, each with an implicit datum supplied by internal

constraints, and explicit constraints supplied by the lens distortion parameters from the plumb line data. In no case were there significant high order additional parameters, most probably due to the relatively narrow fields of view for all cameras. The new principal point position was then adopted for the re-computation of the plumb line data set. The target field network was then re-computed as before. In one or two cases the iterative process had to be continued, either because the principal point location was significantly shifted from the centre of frame, or because of oscillation of the parameters. No significant changes to the calibration parameters, other than the lens distortions, was the convergence criterion used. An integrated solution should alleviate problems with poor initial estimates or parameter oscillation.

6. RESULTS AND ANALYSIS

The results of the processing of the calibration data sets using the combined technique are shown in Table 2. The RMS image errors and relative precisions (the ratio of the mean target coordinate precision to the longest dimension of the object) are results for the target field networks with lens distortion constraints. The improvement of relative precision with larger sensor resolutions is clear, caused by the decrease in the raw angular resolution of the sensor. However, there is no apparent improvement in RMS error (in terms of pixels) with increasing target image size, contrary to results predicted by other investigations (Trinder, 1989; Shortis et al, 1994). The RMS image errors for the plumb line calibrations were, in general, consistently larger than the target field results, due to the smaller span of pixels of the plumb line images. As could be expected (see Figure 2), the difference decreases for the higher resolution sensors.

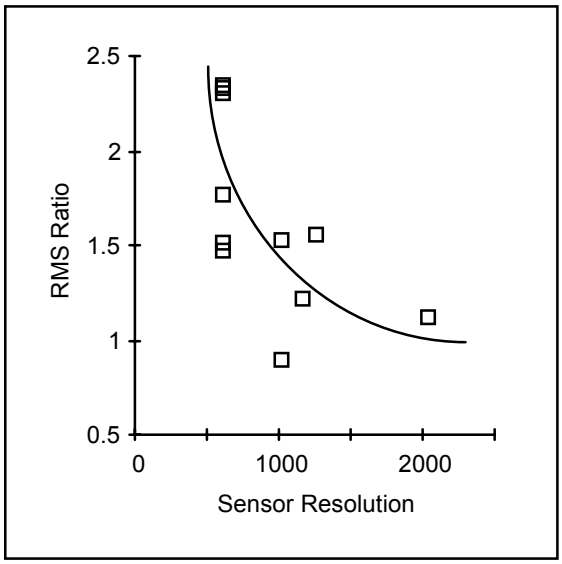

Figure 2. Ratio of the plumb line RMS image error to the target field RMS image error.

CCD Camera	Focal Len. (mm)	RMS Error (um)	RMS Error (pix.)	Relative Precision
Elmo	15	0.30	1/31	1:32000
Sony	12.5	0.30	1/30	1:33000
Cohu analogue	12.5	0.68	1/18	1:26000
Cohu digital	12.5	0.47	1/27	1:30000
Hitachi	12.5	0.42	1/29	1:31000
Pulnix	12.5	0.47	1/27	1:30000
TI Multicam	12.5	0.34	1/21	1:39000
Thompson	24	0.50	1/38	1:59000
	50	0.75	1/25	1:51000
Kodak 1400	24	0.22	1/30	1:67000
	50	0.35	1/19	1:44000
Kodak 4.2	24	0.65	1/14	1:53000
	50	0.36	1/25	1:93000
Kodak DCS200	28	0.40	1/23	1:59000

Table 2. Results of the CCD camera calibrations.

The results for the cameras with the low resolution CCD sensors are remarkably consistent, with the exception of the Cohu analogue camera. Regardless of the format or read-out type of the sensor, RMS image errors and relative precisions are clustered around 1/30 of a pixel and 1:30,000 respectively. The performance of the Cohu analogue camera in this experiment is contrary to previous experience with the camera, which would indicate a routine RMS error in the region of 1/25 of a pixel. Further investigation is required to determine the source of the problem for this camera. The digital transfer system of the Cohu camera is clearly not a significant advantage, compared to the other cameras with similar sensors and analogue output.

The Texas Instruments Multicam shows some improvement over the low resolution sensors in terms of relative precision, but the RMS image error is significantly degraded. Although it is the case that the faster read-out rate reduces the signal and generates higher noise levels, further testing is needed to clarify this result. In particular, a test of the Multicam in the standard mode would be a useful comparison with the results gained here.

The three scientific CCD sensors show mixed results, irrespective of the clear improvement in the relative precisions compared with the low resolution cameras. The Thompson sensor shows the smallest RMS error in the image, in terms of pixels, which is probably partly due to the high radiometric resolution of the sensor. The poorer image space RMS of the Kodak 1400 sensor is offset by the slightly higher sensor resolution. The result for the Kodak 4.2 camera with the 24mm lens is clearly degraded, in comparison to the other sensors, by the read-out noise. At a RMS image error of 1/30 of a pixel, the potential relative precision for this camera is better than 1:110,000. The 50mm Nikkor lenses used for the scientific CCD cameras show consistently weaker results in terms of absolute image space resolution. Ignoring the Kodak 4.2 results because of the read-out noise, the results are significantly degraded when compared to the 24mm lenses. This phenomenon is also worthy of further investigation.

The result for the Kodak DCS200 still video camera was also clearly degraded, in this case by the double re-processing

of the raw pixel values from the sensor. Other experimental testing with this camera has clearly indicated relative accuracies of around 1:70,000 (Fraser and Shortis, 1995). At a RMS image error of 1/30 of a pixel, the potential relative precision for this camera is approximately 1:75,000 according to the testing carried out in this experiment.

Figure 3 shows the derived radial distortion profiles for the two groups of cameras tested with the same lens. The consistency of the profiles is clear, despite probable variations in focus. For the group of four low resolution cameras, the total range of values at a radial distance of 4mm is 1.6um, compared with the expected precision of the profiles of 1.0um at a 95% confidence interval. In contrast, variations of up to 10um were experienced with target field or plumb line calibrations alone. There was similar consistency for the decentring distortion profiles, although the magnitude of the distortion was much less.

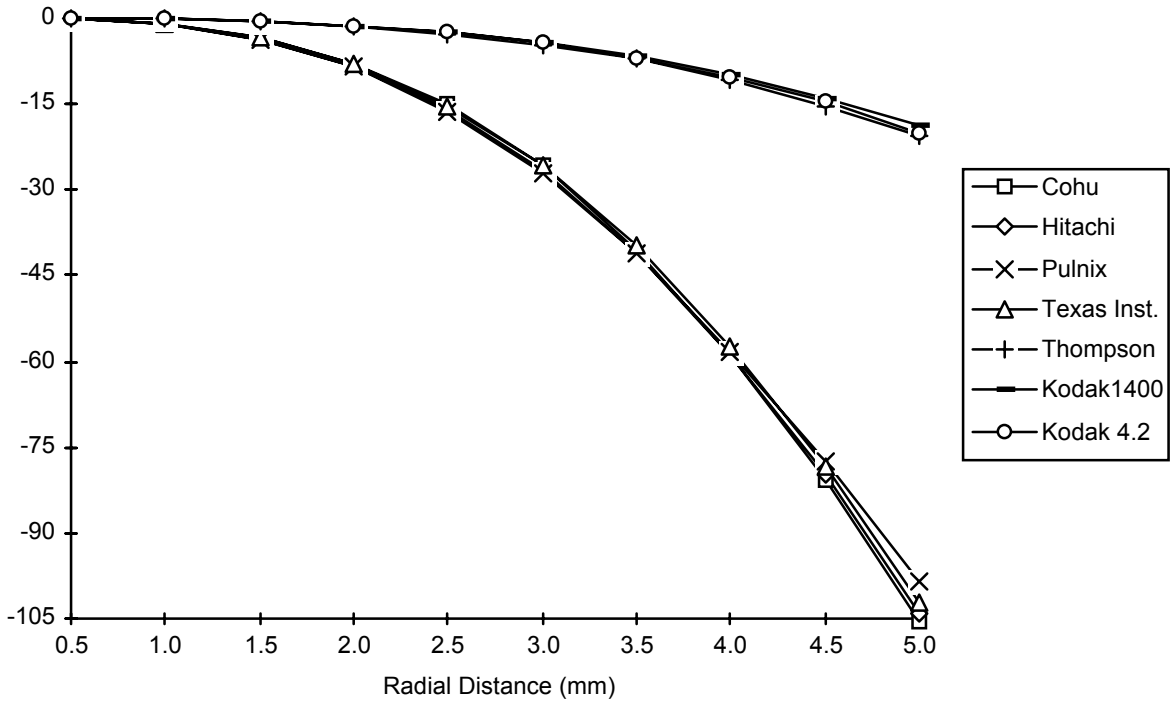

Figure 3. Comparisons of radial distortion profiles.

The test of consistency of the affinity and orthogonality terms for the sensors also indicated a clear consistency for some affinity terms. Results for the two Kodak cameras are shown in Table 3. In both cases the affinity terms derived for the sensors, from calibrations with different lenses, were statistically identical at a 95% confidence level (a one dimensional test is appropriate because of very small correlations with other parameters). Unfortunately the testing of orthogonality for all cameras and affinity for the Thompson camera was less valid because the parameters were only marginally significant or were insignificant.

CCD Camera	Focal Length (mm)	Affinity Term ($x10^4$)	Difference ($x10^4$)	Variance ($x10^8$)	Significance
Kodak 1400	24	2.1911	0.0680	0.0625	0.27
	50	2.1231			
Kodak 4.2	24	6.8139	0.5053	0.1681	1.23
	50	6.3086			

Table 3. Comparisons of affinity terms.

7. CONCLUSIONS

This paper has described an experiment in which fourteen different CCD sensor and lens combinations were calibrated under similar circumstances. The results indicate that under the conditions of high signal to background images, simple thresholds and target image location by centroiding, similar CCD cameras will produce essentially the same level of precision, regardless of the format, sensor read-out type or signal transmission method. This conclusion is very clear for the low resolution sensors. Despite some degradations of the results for the medium and high resolution sensors, it is also clear that increasing image space resolution of the sensor produces the well established trend of improvement in relative precision in the object space. In four cases, cameras gave atypical results. Two of these cases were due to known degradations, whilst the remaining two cases are worthy of further investigation. Finally, the independence of parameters using the technique of combined plumb line and target field calibrations was demonstrated by consistent

lens distortion profiles derived from calibrations of the same lenses mounted on different CCD cameras, and by consistent affinity values for the same sensors and different lenses.

8. ACKNOWLEDGMENTS

This research was partly carried out whilst Mark Shortis was on a research visit at the NASA Langley Research Center sponsored by the Australian Department of Industry, Trade and Commerce. The authors acknowledge with appreciation the loan of the Megaplus 4.2 and DCS200 cameras by Kodak U.S.A.

9. REFERENCES

BEYER, H. A., 1987. Some aspects of the geometric calibration of CCD cameras. Proceedings, International Society for Photogrammetry and Remote Sensing Intercommission Conference on the Fast Processing of Photogrammetric Data, Interlaken, Switzerland, pp 68-81.

BÖSEMANN, W., GODDING, R., and RIECHMANN, W., 1990. Photogrammetric investigation of CCD cameras. Proceedings, SPIE Vol. 1395 Close Range Photogrammetry Meets Machine Vision, Zurich, Switzerland, pp 119-126.

BROOKS, J.D. and BEAMISH, J.K., 1977. Measurement of model aeroelastic deformations in the wind tunnel at transonic speeds using stereophotogrammetry. NASA Technical Paper TP-1010, 41 pages.

BROWN, D. C., 1971. Close range camera calibration. Photogrammetric Engineering, 37(8) : 855-866.

BURNER, A. W., SNOW, W. L. and GOAD, W. K., 1985. Close range photogrammetry with video cameras. Proceedings, Technical Papers, 51st American Society of Photogrammetry Annual Meeting, Washington, U.S.A., pp 62-77.

BURNER, A. W., SNOW, W. L, GOAD, W. K. and CHILDERS, B. A., 1987. A digital video model deformation system. Proceedings, International Congress on Instrumentation in Aerospace Simulation, Williamsburg, U.S.A., pp 210-220.

CASE, J. B., 1961. The utilization of constraints in analytical photogrammetry. Photogrammetric Engineering, 27(5) : 766-778.

CHILDERS B. A., SNOW, W. L., JONES, S. B., FRANKE, J. M. and SHORTIS, M. R., 1994. Support of wake vortex detection research in flight and wind tunnel testing using videometric techniques. Proceedings, International Society for Photogrammetry and Remote Sensing Commission 5 Inter-Congress Symposium, Melbourne, Australia, pp 41-46.

EARLS, C. J., 1983. Accuracy potential of a system for analytical close range photogrammetry. Photogrammetric Record, 11(62) : 169-182.

FAIG, W., and SHIH, T. Y., 1988. Functional review of additional parameters. Proceedings, Technical Papers Volume 3, ACSM-ASPRS Annual Convention, St. Louis, U.S.A., pp 158-168.

FRASER, C. S., 1986. Microwave antenna measurement by photogrammetry. Photogrammetric Engineering and Remote Sensing, 52 (10) : 1627-1635.

FRASER, C. S. and SHORTIS, M. R., 1992. Variation of distortion within the photographic field. Photogrammetric Engineering and Remote Sensing, 58 (6) : 851-855.

FRASER, C.S. and SHORTIS, M. R. , 1995. Metric exploitation of still video imagery. In press for Photogrammetric Record,15(85) : April 1995.

FRYER, J. G. and MASON, S. O., 1989. Rapid lens calibration of a video camera. Photogrammetric Engineering and Remote Sensing, 55(4) : 437-442.

GUSTAFSON, P. C., 1988. The application of real-time and near real-time photogrammetry in industry : A test of accuracy. Proceedings, Commission 5, 16th Congress of the International Society for Photogrammetry and Remote Sensing, Kyoto, Japan, pp 198-205.

HENTSCHEL, M. J. and SHORTIS, M. R., 1991. Calibration of cameras under operational conditions. The Australian Surveyor, 36(1) : 61-74.

LENZ, R., 1987. Lens distortion corrected CCD-camera calibration with co-planar calibration points for real-time 3D measurements. Proceedings, International Society for Photogrammetry and Remote Sensing Intercommission Conference on the Fast Processing of Photogrammetric Data, Interlaken, Switzerland, pp 60-67.

MERCHANT, D. C. and TUDHOPE, R. L., 1989. Aerial photo system calibration over flat terrain. Photogrammetric Engineering and Remote Sensing, 55(12) : 1755-1763.

SHORTIS, M. R., 1988. Precision evaluations of digital imagery for close range photogrammetric applications. Photogrammetric Engineering and Remote Sensing, 54 (10) : 1395-1401.

SHORTIS, M. R., 1989. Industrial photogrammetry at the NASA Langley Research Center. Proceedings, Symposium on Surveillance and Monitoring Surveys, University of Melbourne, Australia, pp 218-231.

SHORTIS, M. R., BURNER, A. W., SNOW, W. L., and GOAD, W. K., 1991. Calibration tests of industrial and scientific CCD cameras. Invited Paper (Paper 6, Volume 1), First Australian Photogrammetric Conference, Sydney, Australia, 12 pages.

SHORTIS, M. R., CLARKE, T. A. and SHORT, T., 1994. A comparison of some techniques for the subpixel location of discrete target images. Videometrics III, SPIE Vol. 2350, pp 239-250.

SHORTIS, M. R. and HALL, C. J. 1989. Network design methods for close range photogrammetry. Australian Journal of Geodesy, Photogrammetry and Surveying, 50 : 51-72.

SHORTIS, M. R., SNOW, W. L., CHILDERS, B. A. and GOAD, W. K., 1993. The influence of storage media on the accuracy and repeatability of photogrammetric measurements using CCD cameras. Videometrics II, SPIE Vol. 2067, pp 80-92.

SNOW, W. L., CHILDERS, B. A. and SHORTIS, M. R., 1993. The calibration of video cameras for quantitative measurements. 39th International Instrumentation Symposium, Albuquerque, New Mexico, May 1993, 28 pages.

TRINDER, J. C., 1989. Precision of digital target location. Photogrammetric Engineering and Remote Sensing, 55 (6) : 883-886.

WILEY, A. G. and WONG, K. W., 1995. Geometric calibration of zoom lenses for computer vision metrology. Photogrammetric Engineering and Remote Sensing, 61 (1) : 69-74.